

Simple Link Atom Saccharide Hybrid (SLASH) Treatment for Glycosidic Bonds at the QM/MM Boundary

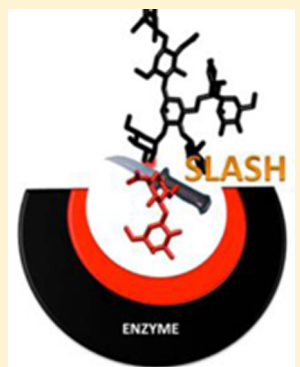
Werner Crous,^{†,‡} Martin J. Field,[§] and Kevin J. Naidoo*,^{†,‡}

[†]Scientific Computing Research Unit and [‡]Department of Chemistry, University of Cape Town, Rondebosch 7701, Western Cape, South Africa

[§]Institut de Biologie Structurale – Jean-Pierre Ebel CEA/CNRS/UJF, 41, rue Jules Horowitz, 38027 Grenoble Cedex 1, France

Supporting Information

ABSTRACT: We investigated link atom approaches for treating the polar C–O bond with particular reference to the glycosidic bond found in complex carbohydrates. We show that cutting this bond after the oxygen in the QM region and saturating the QM system with a hydrogen link atom leads to greater conformational and configurational accuracy at the boundary compared with cutting the bond before oxygen and saturating the QM system with a halogen link atom to represent the oxygen. Furthermore, we find that balancing the MM atom charges and redistributing the boundary atom charges at the QM/MM boundary minimizes the effect of the link atom, both energetically and structurally. This is illustrated via a series of calculations on a set of carbohydrate and carbohydrate-like model compounds. Finally, we confirm the validity of our model by performing molecular dynamics simulations for a typical disaccharide model compound in water. Our postsimulation conformational and configurational analyses show that the oxygen-to-water hydrogen pair distribution functions and the Φ, Ψ distributions at the glycosidic boundary between the quantum and classical regions compare favorably with results obtained from complete QM and complete MM treatments of the saccharide.



1. INTRODUCTION

Cutting a covalent bond in a hybrid quantum-classical potential is often inevitable in quantum mechanical (QM)/molecular mechanical (MM) simulations, and, as such, their treatment is central in the formulation of QM/MM methods. Unfortunately the main focus in developing new partitioning methods has been on carbon–carbon single bonds, and consideration of polar bonds at the QM/MM boundary has received little attention. In chemical glycobiology simulations however, severing at polar bonds is almost an inevitability. This area of chemical biology focuses on the roles played by carbohydrates/glycans, which are ubiquitous in cellular and molecular biology. Indeed a major goal of chemical glycobiology is the discovery of reaction mechanisms of glycoenzymes (i.e., glycotransferases and glycosidases) that are key to glycan biosynthesis and hydrolysis in cellular systems. Therefore the development of simulation tools for use in chemical glycobiological investigations is a priority as it will contribute to advances in fields as diverse as drug discovery¹ and the development of biofuels as alternative energy sources.²

Computer simulations comprising QM/MM potentials are powerful tools for the study of enzyme reaction mechanisms.³ In these approaches, only the chemically active region is treated at the QM level, while the environment is represented with a MM description that is theoretically less accurate. To ensure chemical accuracy in the simulation, amino acid side chains that facilitate or participate in the catalytic reaction require inclusion in the QM region. The protein is then split between QM and

MM regions (Figure 1), where a covalent bond connects QM and MM atoms at the boundary.

A common approach to treating covalent bonds at the QM/MM boundary is the link atom method^{3b} where an extra atom (usually hydrogen) is introduced into the QM region, at a suitable distance along the broken quantum bond, thereby saturating the missing valence of the QM subsystem. Alternative approaches rely on the formulation of atoms with mixed QM and MM character. An example of this is the GHO method in which the MM atom at the boundary is replaced by a pseudo QM atom with sp^3 hybrid orbitals.⁴ Although quite different in principle, these methods share the property that they have almost always been optimized for the treatment of nonpolar carbon–carbon single bonds, as this is usually sufficient for the QM simulation of side chains in protein systems.

Glycoenzymes that biosynthesize branched oligosaccharides in the cell's cytoplasm present unique problems for QM/MM boundary methods. These enzymes physically interact with at least three linked monosaccharides during catalysis so requiring multiple sugar rings to be present inside the catalytic domain to ensure accurate modeling. Only the participating pyranose rings about the forming or breaking glycosidic bond (i.e., the glycosidic bond on the far left in Figure 1) require a quantum representation, while the rest of the saccharide to which it is bonded can be modeled with a classical potential.

Received: October 17, 2013

Published: March 12, 2014



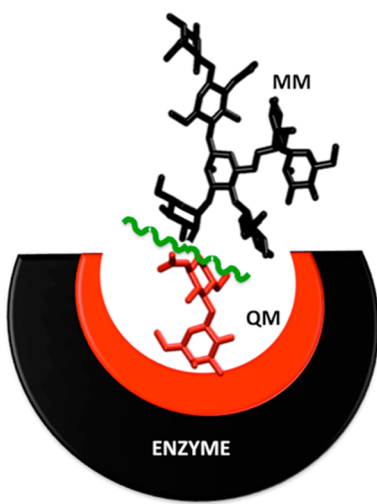


Figure 1. A typical oligosaccharide lodged into a schematic representation of a glycoenzyme catalytic domain. The line squiggle represents the ambiguity faced when attempting to partition the oligosaccharide into quantum mechanically treated (colored red) reacting saccharides (QM) and classically treated (colored black) saccharides of conformational significance.

The difficulties associated with partitioning an oligosaccharide into QM and MM region are illustrated in a recent reaction dynamics simulation of the hydrolysis of cellooctaose.⁵ In place of a computational algorithm designed to partition the glycosidic polar bond we employed a large QM region that contained the two sugar rings on either side of the reactive glycosidic bond and used the GHO method to saturate the +2 and -2 glycosidic linkages. Other ad hoc solutions to partitioning glycosidic bonds use hydrogen link atoms thereby cutting the carbohydrate ring in the MM region and saturating the open QM valences with 2 hydrogen link atoms.⁶ The GHO method is perhaps more theoretically appealing than that of link atoms, but its application to polar bonds suffers from the formal charge condition (FCC) error.⁷ Nevertheless, all of these methods are generally used without due consideration of the disturbing effect they may have on the geometries and conformations of the saccharide and the perturbation caused to the electron density in the QM region.

There are several complications that impede the development of boundary atom methods for polar bonds.⁸ However, such a method is essential for the accurate QM/MM simulation of glycoenzymes and related proteins that are central to chemical glycobiology research. Recently, there have been attempts at developing link atom methods for polar bonds.⁹ Here we report a Simple Link Atom Saccharide Hybrid (SLASH) method as an approach that can be implemented seamlessly into both semiempirical and *ab initio* QM/MM programs. We test the method in QM/MM computations and show that it maintains the conformational and configurational preferences of molecular systems when they are treated entirely at the QM or MM levels of theory, thus improving the accuracy of simulations necessary for glycobiological research.

2. IMPLEMENTING A LINK ATOM TO SACCHARIDES

Link atom methods have the advantage of simplicity of implementation, and, for this reason, they have been implemented in a large number of modeling packages, including AMBER,¹⁰ CHARMM,¹¹ DYNAMO,¹² and GRO-

MOS.¹³ In this work, we employ the CHARMM¹¹ and DYNAMO¹² programs and focus on QM/MM potentials that use semiempirical QM methods.

Important points to consider in a link atom implementation to a glycosidic linkage that joins quantum and classical potentials (i.e., QM-O-MM) are as follows: i) whether to cut the QM-O bond or the O-MM bond; ii) what the location of the link atom should be along the cut bond; iii) how the electrostatic interactions at the boundary should be treated; and iv) how the charges of the bonded MM subsystem should be balanced.

2.1. Cutting a Glycosidic Bond. A bond segregating quantum and classical potentials involves a QM partner (QP), the link atom, (Link), and a boundary atom (BA) that borders the MM region. In addition the MM atoms that are directly bonded to the BA are denoted M2 atoms, while those that are two bonds away are denoted as the M3 atoms (see Figure 2).

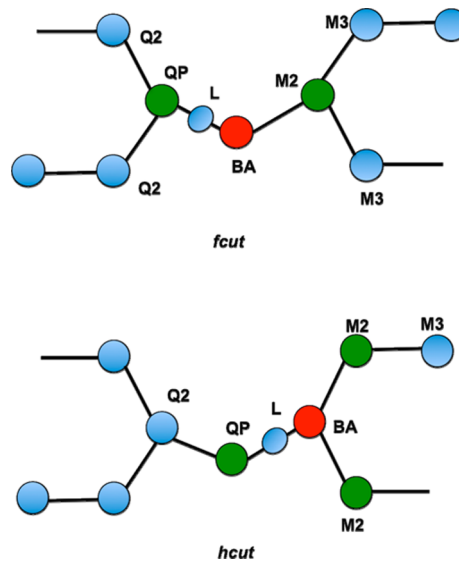


Figure 2. A diagram illustrating the *fcut* and *hcut* approaches to treating a glycosidic linkage boundary region. The boundary atoms are shown in red and the QM partners as well as the M2 atoms in green. The link atom is labeled L.

In this work we considered two approaches to severing the glycosidic linkage which we denote *fcut* and *hcut*. In *fcut*, the glycosidic oxygen is the boundary atom and the link atom, which is a fluorine atom, is positioned between the carbon QP and the glycosidic oxygen BA. We chose a fluorine link atom for *fcut* since it gave better results than a chlorine link atom (it is computationally unfeasible to use larger halogens such as bromine as link atoms). See Supporting Information Tables S1 and S2 for a comparison between the implementation of these two halogens in *fcut*. In *hcut*, the MM carbon atom is the BA, and the link atom, which is hydrogen, is positioned between the glycosidic oxygen QP and the carbon BA.

We also tested the *fcut* approach but with a hydrogen link atom, but this was shown to poorly represent the more electronegative oxygen (see Supporting Information Tables S1 and S2). Saturating a QM oxygen atom with a fluorine link atom is not an efficient procedure since the oxygen as well as the fluorine atoms need to be treated at the QM level of theory leading to computationally more demanding calculations. In addition the standard O-F bond length is poorly defined.

Placing a quantum mechanically treated fluorine next to a quantum mechanically treated oxygen has previously been shown, by others, to give large signed errors.^{9a}

2.2. Relative Link Atom Boundary Position. The most common link atom placement is along the bond with the simplest being a superposition onto the boundary atom. This placement has the disadvantage that extensive parametrization of the link atom may be required to ensure that it has the same chemical behavior as the boundary atom. A more practical approach is to place the link atom somewhere along the QM-MM bond. The position of the link atom, \vec{R}_{link} , is then determined from the positions of the QM partner, \vec{R}_{QP} , and boundary atom, \vec{R}_{BA} , as

$$\vec{R}_{link} = \vec{R}_{QP} + d \frac{(\vec{R}_{BA} - \vec{R}_{QP})}{|\vec{R}_{BA} - \vec{R}_{QP}|} \quad (1)$$

where d is the distance along the bond, and \vec{R} denotes a position vector. Link atom methods that employ eq 1 are well-defined and can be used in geometry optimization and molecular dynamics simulations. Forces on the link atom arising from the QM calculation are straightforwardly transferred to the QM partner and boundary atom.¹⁴

Two methods are common for determining d . In the constant distance method, d is fixed at a value that depends uniquely upon the chemical identity of the link atom and the QM partner. By contrast, in the constant ratio method, d varies and is determined as a given fraction of the actual distance between the boundary atom and QM partner at each minimization or dynamics step. This fraction is calculated based upon a fixed ratio which can either be the ratio of bond lengths in the force field or the ratio of generally accepted bond lengths for the QM partner to the link atom and the QM partner to the boundary atom.⁷

2.3. Electrostatic Interactions at the Boundary. The presence of unscreened MM point charges near the QM region leads to overpolarization of the QM subsystem. The simplest way to address overpolarization is to omit certain of the QM/MM electrostatic interactions as the default Z2 method does for the ONIOM QM/MM potential in the Gaussian program.¹⁵ A pertinent example to this work is the EXGROUP option in the CHARMM program,¹¹ where the charges of a user defined MM atom group are set to zero. Both these approaches modify only the electrostatic interaction between the QM and MM subsystems, while the MM/MM electrostatic interactions remain unchanged. These zero charge methods have been shown to lead to large errors.^{9a}

An improvement on the zero charge method is to preserve the positions of the MM charges but damp the QM/MM interactions by smearing the MM charge distribution using Gaussian¹⁴ or Slater-type s-orbital^{9b} forms. In this work we use a redistributed charge (RC) scheme where the MM charge is shifted away from the BA into the surrounding MM region.^{9,16} In the original RC method¹⁶ the BA charge, q_{BA} , is divided equally among the midpoints of the bonds between the BA and the M2 atoms. A variation of the RC method is the RCD method¹⁶ which partitions q_{BA} between the M2 atoms and the midpoints of the BA-M2 atom bonds aiming to preserve the bond dipole. Variations of the RC method of relevance to this work are the RC2^{9a} and RC3^{9b} methods where q_{BA} is divided between the M2 atoms and q_{BA} is divided between the M2 and M3 atoms, respectively. In this work, we propose an adaptation of the RC algorithm, RC75, in which q_{BA} is distributed three-

quarters, instead of half, the way along the bonds between the boundary and M2 atoms.

In addition we also consider an adaptive RC (ARC) algorithm, in which the way the charge is moved is based upon the chemical environment of the M2 and M3 atoms. The RC algorithm is a special case of ARC in which the charges of the M2 atoms have the same value. This is similar to Jung et al.⁷ who suggested that the auxiliary orbital charge in the GHO method depends upon the hardness of the M2 atoms. In our case we define a distribution operator that employs the absolute differences between the boundary atom charge, q_B , and those of the M2 atoms, q_i . The distributed charge, q_{Bi} , between the boundary atom and one of its MM partners is defined as

$$q_{Bi} = f_i q_B; \quad f_i = \frac{|q_B - q_i|}{\sum_i |q_B - q_i|} \quad (2)$$

2.4. Balancing the Charges of the MM Subsystem. A key consideration when implementing a QM/MM partition is the preservation of total charge of the system. The QM regions in link atom methods have zero or integer charge, and so the charge on the MM subsystem should also be zero or have an integer in complement with that of the QM region. In the case of popularly used force fields such as CHARMM22¹⁷ and OPLS-AA¹⁸ the MM charge distribution has been parametrized in such a way that when partitioning at a carbon–carbon bond the zero or integer charge constraint is fulfilled. However, this is often not the case for other force fields or when polar bonds are being partitioned, and so additional charge readjustments are needed.

To partition the polar bonds about the glycosidic linkage we investigated two algorithms. In Balance Algorithm 1 (BA1) the boundary atom charge is changed to fulfill the constraint, whereas in Balance Algorithm 2 (BA2) the charge of the boundary atom is kept but the M2 atom charges are equally incremented or decremented to conserve the total charge of the system. In the case of the CHARMM27 force field used here only the charges of non-hydrogen atoms in BA2 were modified, with the charges of hydrogens maintained at the values prescribed by the force field.

3. COMPUTATIONAL DETAIL

We investigated the choices of the semiempirical QM parameters for link atoms, implemented at the glycosidic linkage, using a test suite comprising the eleven molecules shown in Figure 3. The molecules were selected to be representative of carbohydrates and carbohydrate-like systems, with special emphasis on model compounds that are pertinent for studies in mammalian cancer glycobiology.¹⁹

The choice of boundary atom methods should not interfere with the saccharide's conformational alignment and electrostatic profile inside the catalytic domain of an enzyme as these molecular systems feature key hydrogen-bonding patterns with the surrounding protein. To ensure the preservation of this and other properties, we included calculations on 13 deprotonated forms of the test molecules, with the relevant protons that were removed indicated by asterisks in Figure 3. We denote the deprotonated forms of the molecule with a “d”, and for compounds m2 and m3 that have two deprotonation sites, we use “d1” for the site nearest to the QM/MM boundary and “d2” for that furthest away.

The reference structures for each compound, including the deprotonated forms, were obtained by optimizing the geo-

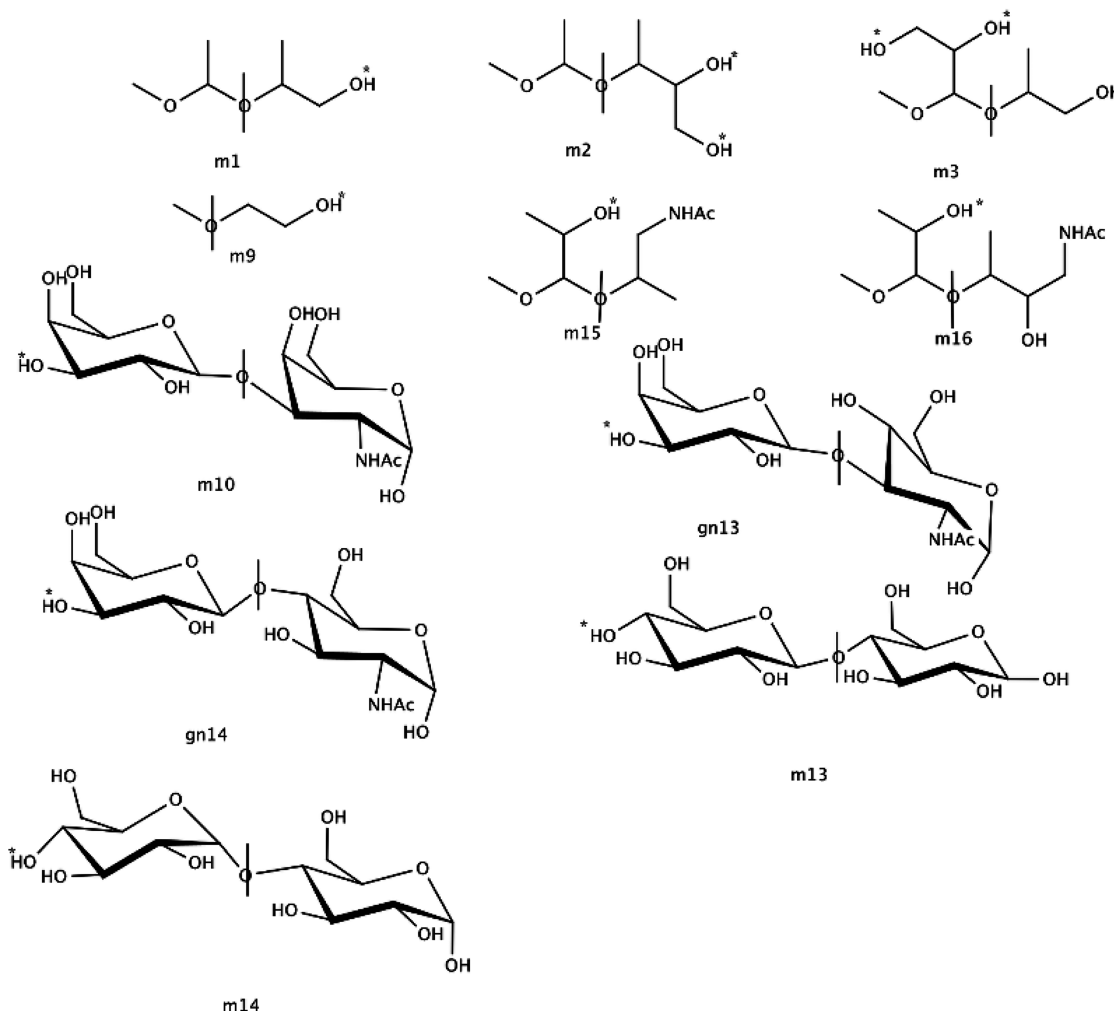


Figure 3. Protonated forms of the model compounds used in the study. The vertical line through the oxygen represents the QM/MM division. For compounds m1, m2, and m9, the QM region is on the right, whereas for all the rest the QM region is on the left. Asterisks denote the protons that are removed in the deprotonated forms of the molecules.

metries with a semiempirical level of theory. Since phosphates are central to glycosylation, we only used semiempirical methods that are able to reliably model hypervalent phosphoric systems. Therefore we choose to implement the SLASH method in SCC-DFTB²⁰ and a modified version of AM1/d-PhoT²¹ because of their reliability in computations that involved phosphates. We used a modified AM1/d-PhoT semiempirical parameter set (see Table S8 in the Supporting Information) as it produces improved carbohydrate ring puckered performance^{21a} compared with the original AM1/d-PhoT parameters.^{21b} This was achieved from a partial reparameterization of the carbon atom. We will for the sake of simplicity refer to this as the AM1/d-PhoT method from now on. In all QM/MM calculations the CGENFF force field²² or the CSFF²³ force field were used to perform the classical (MM) modeling.

Molecular dynamics simulations of the m10 model system (see Figure 3) in water were carried out with a modified AM1/d-PhoT QM/MM method implemented in version c35b5 of the CHARMM program¹¹ and its interface to the MNDO97 semiempirical QM package.²⁴ A cubic TIP3P²⁵ water box of side 34 Å was used for condensed phase simulations. The lengths of bonds involving MM hydrogen atoms were constrained using the SHAKE algorithm.²⁶ Electrostatic

interactions were computed using periodic boundary conditions and with a force switching group-based scheme with outer and inner cutoffs of 12 and 10 Å, respectively. Lennard-Jones interactions were calculated in the same way but with a standard shifting function. After an initial minimization and heating phase, constant temperature simulations of 600 ps duration were run for each model.

As a test of the transferability of the link atom methods the MD simulations were repeated for SCC-DFTB²⁷ as implemented in CHARMM. Exactly the same simulation and setup protocols were employed as before. For the SCC-DFTB method itself, we used the mio parameter set, together with on-site diagonal Hubbard derivatives of -0.17 for oxygen, -0.11 for nitrogen, -0.04 for carbon and -0.14 for hydrogen.^{20b} We did not include any empirical E_{cor} corrections for O–C bonds as defined for SCC-DFTB with GHO²⁸ since this option is specific to the SCC-DFTB method implemented in CHARMM and not generally transferable. No dispersion corrections were included, and the ζ -parameter, modifying the hardness of the hydrogen atom, was set to 5.0.

After completion, all simulations were analyzed to determine the Φ, Ψ distributions (see Figure 4 for a definition of the angles) of the glycosidic bond of the model compound. Furthermore we calculated the pair distribution functions for

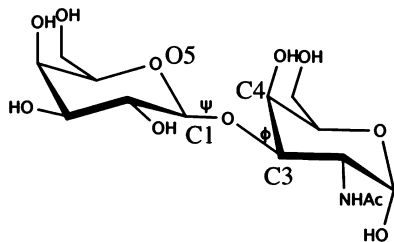


Figure 4. The definition of Φ and Ψ dihedral angles about the glycosidic linkage of a model disaccharide present in chemical glycobiological simulations.

water hydrogens to the QP glycosidic oxygen to determine the configurational consistency of our QM/MM simulations against those with pure QM and pure MM potentials.

4. DEVELOPING AND CONFIGURING SLASH

In section 2 above we surveyed the important considerations for developing a link atom implementation. Here we lay out properties that are important in saccharide QM/MM simulations. The performance of the measures listed below (I–VII) are evaluated for i) the glycosidic linkage cutting position; ii) the location of the link atom along the cut bond; iii) the electrostatic interactions at the boundary; and iv) the treatment of the charges of the bonded MM subsystem.

I. The Mean Unsigned Error (MUE) in charges determined as the difference in the Löwdin charges for the corresponding atoms in QM/MM (excluding the link atom) and QM systems.

II. The average RMSD in the charges between the QM/MM and QM systems as computed in I above.

III. The average RMSD in coordinates.

IV. The change in the length of the partitioned bond relative to the equivalent QM bond.

V. The MUE in the total system dipole moment.

VI. The MUE in the deprotonation energies calculated as the difference in energy between the geometry-optimized protonated and deprotonated forms.

VII. The MUE in the value of the torsion about the bond connecting the QM and MM regions compared with the equivalent QM torsion.

The performances of link atoms in the QM/MM calculations for these properties were compared against full QM calculations. Of the properties deprotonation energies have been shown to be the most challenging to reproduce²⁹ since both the effect of the force field energy terms and the QM energy terms are included, and it is therefore sensitive to the treatment of the boundary.

We started by optimizing hydrogen link atoms from the semiempirical AM1/d-PhoT parameters in a procedure similar to Wang and Truhlar.⁹ The latter authors used a single parameter to tune the pseudopotential, whereas in our study we used a genetic algorithm,³⁰ along with a classic parametrization protocol that included geometry optimization, to tune several parameters with the objective of getting the hybrid QM/MM models to reproduce the properties of the reference quantum models. The deprotonated systems were not included in the parametrization except for the determination of the deprotonation energies in which case the values were attributed to the corresponding protonated forms. The fitness function for the algorithm was calculated as the sum of all the squares of the individual errors for the different properties over all the model

systems in the parameter set. After experimenting with several combinations we arrived at a set of weightings 10, 12, 1, 50, 0, 1, and 0 for properties I to VII, respectively. In so doing the system dipole and QM-MM dihedral angle were omitted from the optimization calculations. Greater weights for properties I, II, and IV were used to emphasize the reference geometries during the parametrization as these were found to be critical in permitting the reproduction of saccharide conformational and configurational condensed phase properties. The model systems in both their protonated and deprotonated forms were fully geometry optimized for the property calculations with each trial parameter set. All model systems, except for m13 and m14, were used in the parametrization. The m13 and m14 molecules were used in the final testing. The starting population for the algorithm contained 128 members, and the optimizations were run in parallel due to their significant computational expense. Further details can be found in Tables S10 and S11 in the Supporting Information.

4.1. Partitioning, Balancing, and Charge Redistribution.

First the different partitioning and balancing methods when using the RC charge redistribution algorithm were compared (see Supporting Information Table S3). We find that the *combination of BA2 balancing and hcut partitioning performs the best* as it produces the optimum results for properties I–V and close to optimum for properties VI and VII. While the best results for properties VI and VII are found using the BA1/fcut model it performs significantly worse for a number of the remaining properties, namely the deprotonation energies and molecular dipole moment. Overall, the BA1/hcut model performs slightly better than BA1/fcut, with BA2/fcut the worst. The differences in these results are mainly due to the differences in using a QM oxygen or replacing it with a fluorine link atom.

To illustrate the effect of changing the charge redistribution and partitioning algorithms, the BA2/hcut and BA1/fcut (Supporting Information Tables S3–S6) models were evaluated. Note that the adaptive models do not apply to fcut since the glycosidic oxygen has only a single MM partner. An overview shows that the BA2/hcut models perform uniformly better than the BA1/fcut models, with the exception of the MUE of the total QM charge which is best for the BA1/fcut/RC2 combination. For the BA2/hcut schemes (in Table S3) the adaptive and nonadaptive schemes give very similar results.

For most of the properties, moving the charge away from the link atom gives worse results, especially for the total QM charge and the deprotonation energies. The exceptions are the molecular dipole moment and the QM-MM dihedral angle for which the RC2 model results are optimum. From this we conclude that RC and ARC perform best, with RC75 giving results that are intermediate between RC and RC2 but closer to RC. This trend is in contrast to the findings of Wang and Truhlar^{9b} where it was observed that moving the charge further away from the fluorine link atoms resulted in improved results. In that case, when the distributed charge is close to the boundary, the charge has to be dispersed to minimize the errors. The BA1/fcut results (Tables S3 and S5 Supporting Information) are not as definitive as the BA2/hcut results (Tables S3 and S6 Supporting Information).

Finally the deprotonation energies for the model systems using hcut partitioning and BA2 balancing and the different adaptive and nonadaptive redistributed charge algorithms (see Supporting Information Table S4) present similar trends with the nonadaptive and adaptive algorithms having comparable

performance. In addition, when the charge distribution is kept close to the link atom, both the RC and ARC models give better performance, with the RC75 and ARC75 results being intermediate between RC2 and ARC2, respectively.

In summary, we find that the choice of hcut partitioning and BA2 balancing outperforms the alternative methods, notably ones that employ fluorine link atoms. Of the redistributed charge algorithms, RC and RC2 both perform best for certain properties.

4.2. Parametrizing the Hydrogen Link Atom. In the comparison between the fcut and hcut approaches the latter was shown to be the most appropriate boundary method for partitioning glycosidic bonds. Subsequently we performed parameter optimization for the hydrogen link atom. In the case of the AM1/d-PhoT semiempirical method, for which there are 15 parameters for hydrogen, the GA produced two parameter sets with very similar fitness. The values of the optimized parameters in these sets are given in the Supporting Information (Table S11), along with other data concerning the optimizations (Table S10).

The full complement of properties I–VII was calculated using the BA2/hcut/RC combination for the two optimized parameter sets as well as the original parameters (Table 1) The

Table 1. Summary of the Results for the Two Hydrogen Link Atom Parameter Sets Produced from GA Optimizations^a

property	original	parameter set 1	parameter set 2
average coordinate RMSD (Å)	0.458	0.474	0.514
average QM charge RMSD (e)	0.027	0.020	0.021
MUE of total QM charge (e)	0.090	0.040	0.060
MUE of QM-MM bond length (Å)	0.010	0.070	0.030
MUE of molecular dipole moment (D)	0.930	0.990	1.010
MUE of deprotonation energies (kcal/mol)	2.970	2.720	2.250
MUE of QM-MM dihedral angle (degrees)	13.81	15.15	16.01

^aCalculations are done with hcut partitioning, BA2 balancing, and RC charge redistribution. The best results for each model are highlighted in bold.

optimized parameter sets 1 and 2 both show improved results for the charge and dipole related properties and the deprotonation energies, but the geometric properties (RMSD, bond length and dihedral angle) are worse compared to the original parameters. The loss in geometric and conformational accuracy of the saccharide glycosidic bond is nontrivial. This is because a major objective is to preserve the conformation of the substrate and its interaction with key amino acids in the enzyme binding pocket or catalytic domain which is central to modeling systems in chemical glycobiology. On balance there appears to be no gain in undertaking the extra complexity associated with using specially parametrized link atoms. Therefore unmodified semiempirical hydrogen parameter sets were selected to refine the SLASH method.

4.3. In Summary. Varying the link atom type, charge redistribution procedure (RCx and ARCx), and charge balancing (BA1 and BA2) to achieve the optimal static properties (electrostatic and geometric) for model systems in the gas-phase allows us now to propose the best combination of procedures that define the SLASH method for glycosidic bonds. The most accurate results for static properties are obtained using the hcut method combined with the BA2 MM

charge balancing method and the RC charge distribution algorithm. RC75 as a charge distribution algorithm performs reasonably and gives results somewhere between that of RC and RC2. The ARCx methods result in minimal gain balanced against the added complexity introduced. This is also the case for parametrizing the link atom.

5. CONDENSED PHASE CONFORMATIONAL AND CONFIGURATIONAL PERFORMANCE

A critical validation step is to measure the extent to which the link atom interferes with the performance of the targeted molecular system in dynamic condensed phase simulations. This is after all the major intent of link atom method development even though it is generally omitted from most development studies, despite recognition of its importance.¹⁶ As a result, we performed condensed phase MD simulations of carbohydrates with a number of boundary atom methods to validate and to further refine the SLASH method for practical implementation. In the previous sections we established from the gas-phase calculations that the best cutting method is hcut and the best MM charge balancing method BA2, and so we only considered this combination in our simulations. Instead we concentrated our efforts on optimizing the charge distribution algorithm.

We compared various implementations of SLASH using hcut partitioning and BA2 balancing to pure QM and MM representations of the model system. Furthermore the performance of other schemes for chemical glycobiological simulations, such as CHARMM's EXGROUP link atom and the GHO method, were used for comparison to SLASH. There are two limitations of the EXGROUP method as it is often used in CHARMM. First, the charges of the group that are zeroed are those of the boundary and the hydrogen atom directly bonded to it. Second, the link atom is allowed to move independently. It is possible to add constraints to keep the link atom on the bond, but this can lead to large forces at the boundary.³¹ A limitation of the GHO method implementation in chemical glycobiological calculations is that the glycosidic oxygen is in the QM region and it is a ring carbon (in this case the C3 atom) of the bond that is treated as the GHO boundary atom with the appropriate parametrization.

Key criteria for boundary methods aimed at the glycosidic linkage are as follows: 1) that the Φ, Ψ distributions are consistent with the QM and MM levels of theory employed; and 2) the bond geometry and water structure around it are preserved. These properties that pertain to the conformational and configurational preferences of the QM and MM regions are central to the accuracy of any boundary model since it should have minimal interference on the "natural" behavior of the QM and MM models. Furthermore the boundary method should not introduce spurious solvent effects that are absent in the MM and QM models.

5.1. AM1/d-PhoT. First we describe the performance of the SLASH implementation in the NDDO semiempirical QM method, AM1/d-PhoT, where the RCx and ARCx calculations were performed with hcut partitioning and BA2 balancing. The Φ, Ψ distributions from MD simulations of the m10 model system in water boxes are shown in Figure 5.

The Φ, Ψ distributions (in Figure 5) are plotted from the highest population (red) to lowest population (blue) from which the QM (Figure 5 a) and MM (Figure 5 b) distributions show reasonable agreement with each other. The former, however, is more diffuse and spreads to larger Φ values. Both distributions have a single broad region with the highest

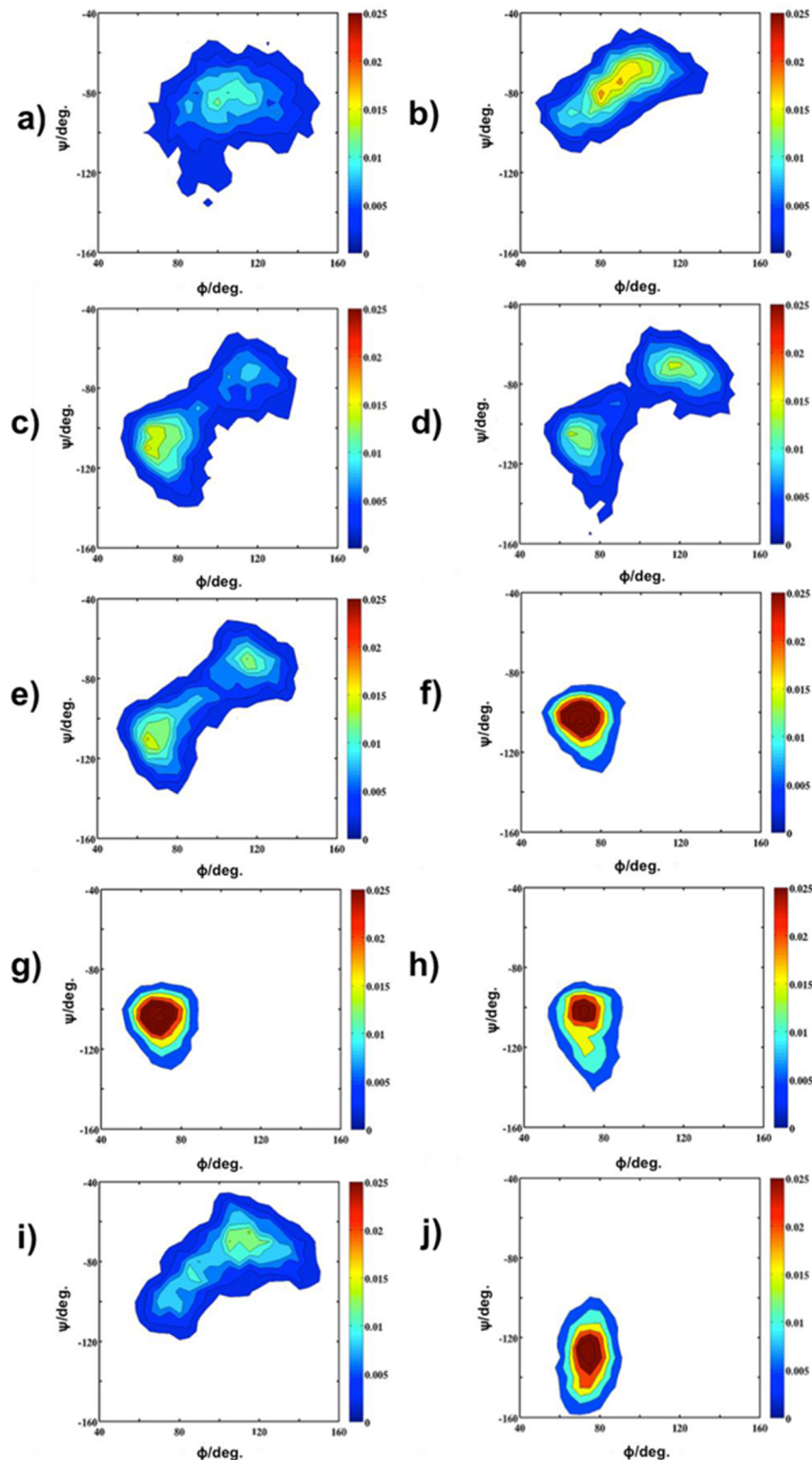


Figure 5. Φ,Ψ distributions obtained for the m10 model system with AM1/d-PhoT as the QM method: a) the model system is treated only as QM; b) only as MM; c) QM/MM with RC charge distribution; d) QM/MM with RC75 charge distribution; e) QM/MM with RC2 charge distribution; f) QM/MM with ARC charge distribution; g) QM/MM with ARC75 charge distribution; h) QM/MM with ARC2 charge distribution; i) QM/MM with the GHO method; j) QM/MM with the EXGROUP CHARMM link atom option.

density. The QM/MM SLASH RC_x distributions cover a similar region of Φ,Ψ space although the sampling population splits into two high density regions centered about the Φ,Ψ angles ($70,-110$) and ($120,-70$). In the case of the RC model

(Figure 5c), the former region is the most sampled, although the sampling population of the second region increases as the charge is shifted away from the QM-MM bond; e.g. RC75 (Figure 5d) compared with RC2 (Figure 5e).

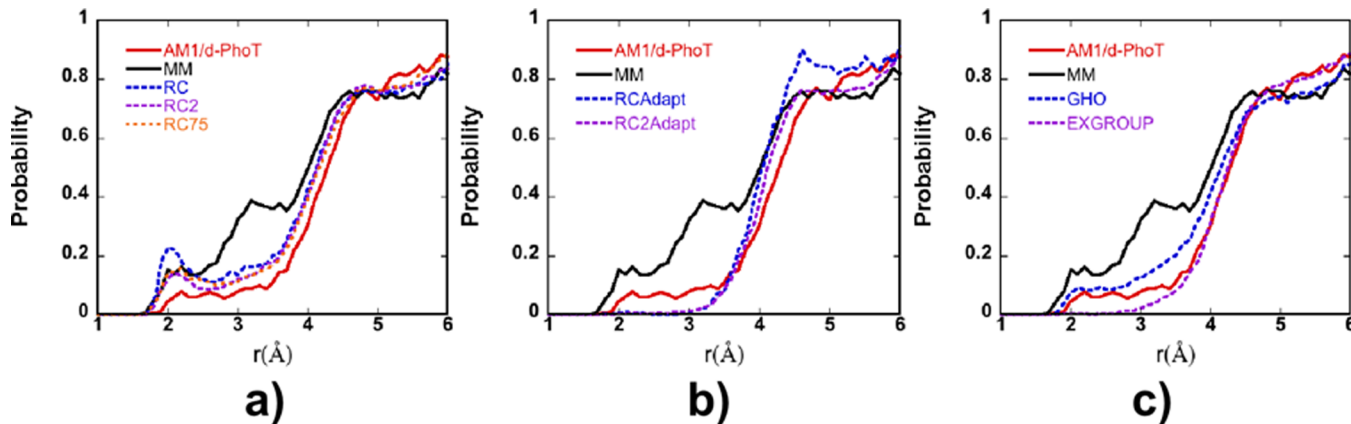


Figure 6. Pair-distribution functions between water hydrogen and glycosidic oxygen for the m10 model system with the AM1/d-PhoT QM method (solid red line) and the MM method (solid black line) compared with the QM/MM implemented a) RC methods, b) the ARC methods, and c) the GHO and EXGROUP methods.

Of the remaining QM/MM boundary methods, GHO produces a distribution that matches the MM distribution and is in reasonable agreement with that from the QM simulation. The ARC and EXGROUP models perform poorly (Figure 5f-h and j) producing highly localized distributions that are centered away from either the QM or MM distributions. The poor performance of the ARC models implies that the charges in the MM-region that are near the boundary must be included in the QM/MM electrostatic interaction for carbohydrates. The EXGROUP suffers the same deficiency and is not suitable for complex carbohydrate modeling.

The pair distribution functions between the glycosidic oxygen and water hydrogens ($g(r)_{O-H_w}$) are shown in Figure 6. Here the saccharide model (m10) when treated as an entirely QM model and then as an entirely MM model, immersed in a classical water model, produces significantly different $g(r)_{O-H_w}$'s in each case. The latter displays much more solvent structure at both short- and long-range distances compared with the QM treatment. When comparing the QM/MM models, the worst performers are the ARC (Figure 6b) and EXGROUP (Figure 6c) models where no solvent structure is visible about the QP glycosidic oxygen atom.

At the other solvent structuring extreme is the RC link atom simulation that produces a peak at short-range that is much larger than the already pronounced MM short-range solvent configurational results. RC75, RC2, and GHO are intermediate between the MM and QM curves, with RC75 most resembling the MM curve and GHO the QM one.

SCC-DFTB. Previously we showed that the SCC-DFTB semiempirical method best reproduces carbohydrate ring pucker^{5a} and is often used in QM/MM simulations involving carbohydrates. Although we did not perform any tests in the gas-phase for this method we did measure transferability of the SLASH method to the often used SCC-DFTB semiempirical method in condensed phase saccharide simulations.

As with AM1/d-PhoT, the SCC-DFTB calculations were performed using an hcut partitioning and BA2 balancing. The MD results obtained for a saccharide SCC-DFTB QM treatment, RCx and ARCx SLASH QM/MM implementations, and a complete MM saccharide treatment are presented in Figures 7 and 8. The QM Φ, Ψ distribution for the complete SCC-DFTB (Figure 7a) treatment of the saccharide is centered about (100, -60) but much more diffuse compared with the case when the saccharide is completely modeled via MM

(Figure 7b). Furthermore the Φ, Ψ distribution gained from the SCC-DFTB model (Figure 7a) is significantly more diffuse than the distribution obtained with the AM1/d-PhoT method (Figure 5a). A further difference is the appearance of a second Φ, Ψ region centered about (100, 180) that is well sampled. As in the AM1/d-PhoT study presented above the SLASH RC implementation in the QM/MM simulation produces a distribution (Figure 7c) that is reasonably compatible with QM and MM saccharide solvent simulations, although it is split into two regions of high density. In the RC75 implementation (Figure 7d) there is a single distribution that is in very good agreement with the MM and SCC-DFTB results, although not as dispersed as the SCC-DFTB Φ, Ψ distribution.

By contrast, the RC2 distribution (Figure 7e) diverges from the MM values resulting in insufficient sampling in the region around (120, -70). The adaptive models, ARC, ARC75, and ARC2, give distributions (Figure f-h) centered at (110, -100) that are far away from either the complete SCC-DFTB or MM treatments. GHO performs reasonably well (Figure 7i) although not as well as it does when implemented within an AM1/d-PhoT QM/MM environment. Finally the EXGROUP implementation in the QM/MM simulation produces a distribution that in no way resembles the complete SCC-DFTB treatment or the complete MM treatment of the saccharide and appears unsuitable in simulations where the glycosidic linkage is severed.

The pair distribution functions from simulations using a complete SCC-DFTB, a complete MM treatment, and QM/MM RCx and ARCx treatments for saccharides immersed in classically modeled water (TIP3P), produced very similar $g(r)_{O-H_w}$ for the QP glycosidic oxygen (Figure 8). The exceptions are the GHO and EXGROUP models that show relatively little short-range solvent structure, with almost all the solvent structure being lost about the QP glycosidic oxygen compared with the complete QM or MM treatments. This is similar to what we observed in the equivalent AM1/d-PhoT simulations. A closer observation reveals that the curves for the adaptive models and RC2 have slightly too much structure at short-range, whereas the RC and RC75 are in good agreement with both the QM and MM results.

The molecular dynamics results of the last two sections show that the SLASH method is capable of reproducing the conformational behavior of a model system and the water structure about the severed glycosidic bond when an

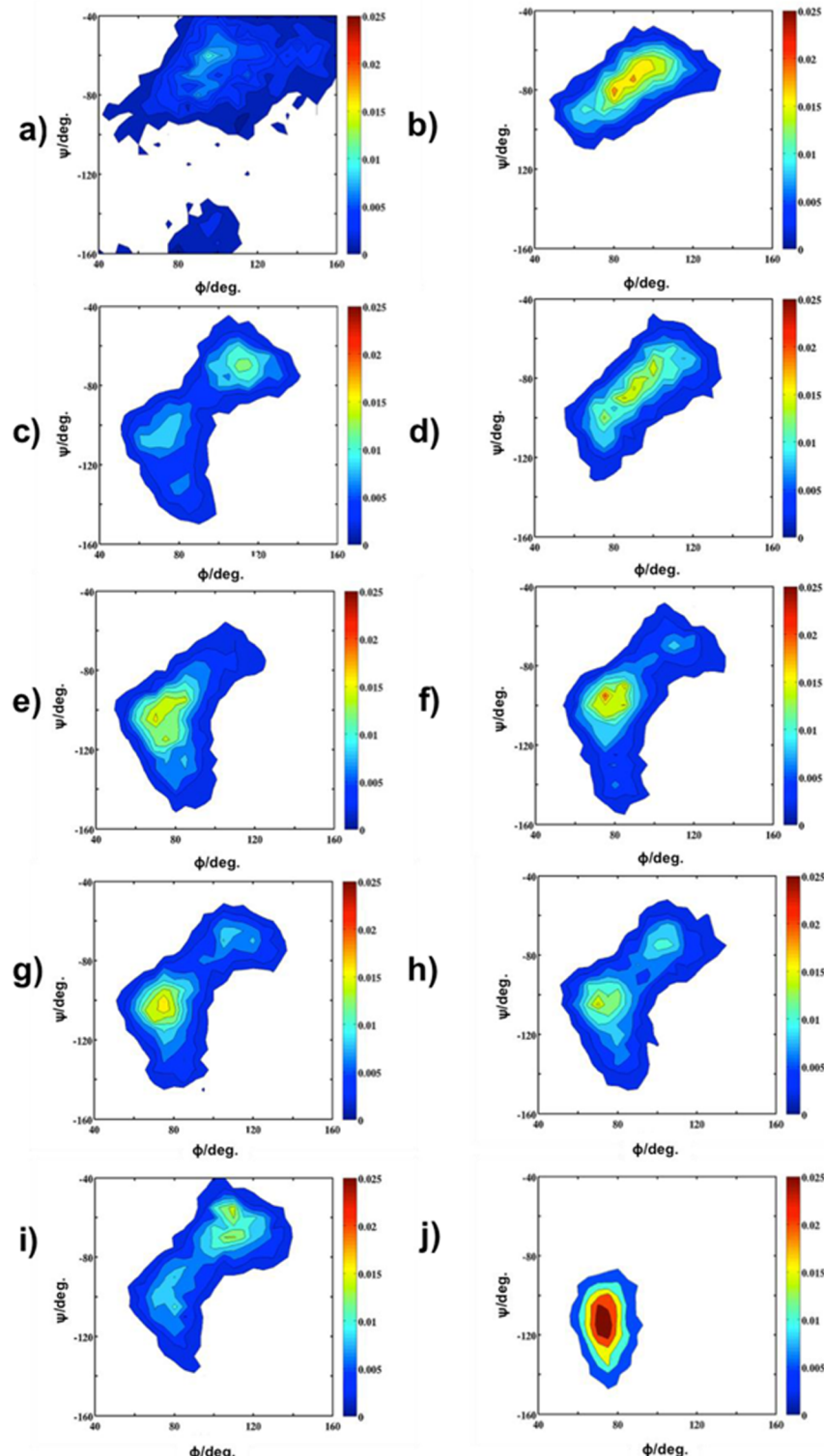


Figure 7. Φ, Ψ distributions obtained for the m10 model system with the SCC-DFTB QM method: a) the model system is treated only as QM; b) only as MM; c) QM/MM with RC charge distribution; d) QM/MM with RC75 charge distribution; e) QM/MM with RC2 charge distribution; f) QM/MM with ARC charge distribution; g) QM/MM with ARC75 charge distribution; h) QM/MM with ARC2 charge distribution; i) QM/MM with the GHO method; j) QM/MM with the EXGROUP CHARMM link atom option.

appropriate redistributed charge algorithm is used. Both RC2 and RC75 appear to produce excellent conformational and configurational behavior compared with nonhybrid (QM or MM) saccharide models. We consider condensed phase performance to be of the greatest importance in the QM/

MM simulation of saccharides, and so our best treatment of glycosidic bonds comprises the following:

- I. Using a hydrogen link atom and cutting the bond after the glycosidic oxygen i.e. the hcutf method.

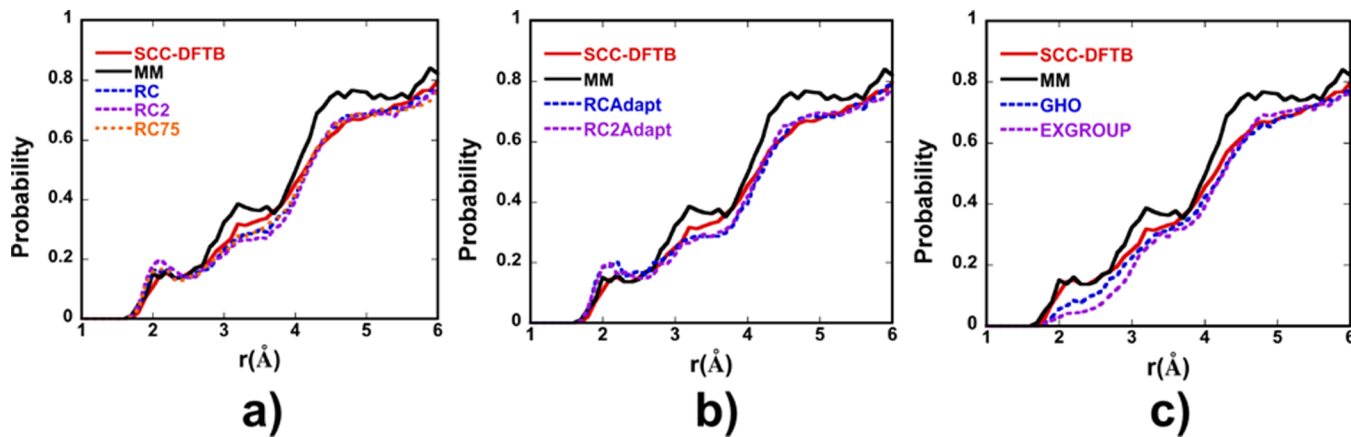


Figure 8. Pair-distribution functions between water hydrogen and glycosidic oxygen for the m10 model system with the SCC-DFTB QM method (solid red line) and the MM method (solid black line) compared with the QM/MM implemented a) RC methods, b) the ARC methods, and c) the GHO and EXGROUP methods.

II. Using the BA2 balancing method in which the charges of the M2 partner atoms are adapted as opposed to those of the boundary atom.

III. Using the RC or RC75 charge distribution algorithm for the QM/MM electrostatic interactions. RC performed slightly better in the gas phase than RC75, although the latter performs marginally better in the condensed phase. However, the differences in performance are small.

6. CONCLUSIONS

In this paper we have investigated link atom approaches for glycosidic linkages in QM/MM simulations of carbohydrates. We considered different link atom types and various charge balancing and redistribution schemes. The optimum method is one in which the glycosidic bond is cut after the QM glycosidic oxygen and the severed bond is saturated with a hydrogen link atom. This, together with appropriate charge balancing and redistribution, comprises the easily implemented and computationally efficient SLASH method.

We found that for glycosidic polar bonds at the QM/MM boundary the hcut, balance algorithm BA2, and charge distributions RC and RC75 produce simulations that least interfere with the QM and MM conformational behavior and the interaction of the glycosidic bond with the surrounding environment. Although developed for carbohydrates, this approach may be transferable to the QM/MM partitioning of systems with similar types of polar bonds. We observed that

1. The retention of the glycosidic oxygen in the QM region and saturation of the QM-MM bond with a hydrogen link atom is more accurate than the alternative of putting the oxygen in the MM region and representing it with a fluorine link atom.

2. Any residual nonzero or nonintegral charge arising from the partitioning of the system can be best accommodated for by modifying the charges of the M2 atoms rather than the boundary atom itself.

3. There is no single redistributed charge method, in which the boundary atom MM charge is moved to neighboring atoms or bonds, that is universally transferable. This is because the position of the boundary charge affects the polarity of the QM-MM bond. Overall, both the RC and RC75 algorithms appear to be suitable for producing conformational and configurational results that are compatible with the case where the saccharide is treated entirely by MM or entirely by QM.

4. Adaptive RC methods, using the adaptation function of eq 2 that is tested here, do not appear to provide an advantage over their nonadaptive alternatives, as they produce a significant loss in geometric and conformational accuracy.

5. Specific parametrization of the link atom QM parameters improves certain properties but causes deterioration in others and does not appear to be beneficial in the general case.

6. The SLASH method is transferable between QM approaches as it was parametrized using the AM1/d-PhoT semiempirical Hamiltonian but then successfully transcribed to the SCC-DFTB QM/MM Hamiltonian.

■ ASSOCIATED CONTENT

S Supporting Information

Tables containing the deprotonation energies and MUE for the link atom models utilizing the AM1/d-PhoT method as well as details regarding the parametrization of the link atom. This material is available free of charge via the Internet at <http://pubs.acs.org>.

■ AUTHOR INFORMATION

Corresponding Author

*E-mail: kevin.naidoo@uct.ac.za.

Notes

The authors declare no competing financial interest.

■ ACKNOWLEDGMENTS

This work is based upon research supported by the South African Research Chairs Initiative (SARChI) of the Department of Science and Technology and National Research Foundation to K.J.N. W.C. thanks SARChI for doctoral fellowship support. The authors thank the France-South Africa cooperation programme grant no. 77964 for travel and stay support.

■ REFERENCES

- (1) Bertozzi, C. R. Chemical glycobiology. *Science* **2001**, *291* (5512), 2357–2364.
- (2) Himmel, M. E.; Ding, S.-Y.; Johnson, D. K.; Adney, W. S.; Nimlos, M. R.; Brady, J. W.; Foust, T. D. Biomass recalcitrance: engineering plants and enzymes for biofuels production. *Science* **2007**, *315* (5813), 804–807.
- (3) (a) Warshel, A.; Levitt, M. Theoretical studies of enzymic reactions: Dielectric, electrostatic and steric stabilization of the carbonium ion in the reaction of lysozyme. *J. Mol. Biol.* **1976**, *103*

- (2), 227–249. (b) Field, M. J.; Bash, P. A.; Karplus, M. A combined quantum mechanical and molecular mechanical potential for molecular dynamics simulations. *J. Comput. Chem.* **1990**, *11* (6), 700–733. (c) Mulholland, A. J. Modelling enzyme reaction mechanisms, specificity and catalysis. *Drug Discovery Today* **2005**, *10* (20), 1393–1402. (d) Mulholland, A. J. Computational enzymology: modelling the mechanisms of biological catalysts. *Biochem. Soc. Trans.* **2008**, *36*, 22–26.
- (4) Gao, J. L.; Amara, P.; Alhambra, C.; Field, M. J. A generalized hybrid orbital (GHO) method for the treatment of boundary atoms in combined QM/MM calculations. *J. Phys. Chem. A* **1998**, *102* (24), 4714–4721.
- (5) (a) Barnett, C. B.; Naidoo, K. J. Ring puckering: A metric for evaluating the accuracy of AM1, PM3, PM3CARB-1 and SCC-DFTB carbohydrate QM/MM simulations. *J. Phys. Chem. B* **2010**, *114*, 17142–17154. (b) Barnett, C. B.; Wilkinson, K. A.; Naidoo, K. J. Pyranose ring transition state is derived from cellobiohydrolase I induced conformational stability and glycosidic bond polarization. *J. Am. Chem. Soc.* **2010**, *132*, 12800–12803.
- (6) (a) Gómez, H.; LLuch, J. M.; Masgrau, L. Substrate-assisted and nucleophilically assisted catalysis in bovine α 1,3-galactosyltransferase. Mechanistic implications for retaining glycosyltransferases. *J. Am. Chem. Soc.* **2013**, *135* (18), 7053–7063. (b) Polyak, I.; Thiel, W.; Masgrau, L. Retaining glycosyltransferase mechanism studied by QM/MM methods: Lipopolysaccharyl-alpha-1,4-galactosyltransferase C transfers alpha-galactose via an oxocarbenium ion-like transition state. *J. Am. Chem. Soc.* **2012**, *134*, 4743–4752. (c) Bowman, A. L.; Grant, I. M.; Mulholland, A. J. QM/MM simulations predict a covalent intermediate in the hen egg white lysozyme reaction with its natural substrate. *Chem. Commun. (Cambridge, U. K.)* **2008**, No. 37, 4425–4427.
- (7) Jung, J.; Choi, C. H.; Sugita, Y.; Ten-no, S. New implementation of a combined quantum mechanical and molecular mechanical method using modified generalized hybrid orbitals. *J. Chem. Phys.* **2007**, *127*, 204102–204112.
- (8) Senn, H. M.; Thiel, W. QM/MM methods for biological systems. *Topics Curr. Chem.* **2007**, *268*, 173–290.
- (9) (a) Wang, B.; Truhlar, D. G. Combined quantum mechanical and molecular mechanical methods for calculating potential energy surfaces: Tuned and balanced redistributed-charge algorithm. *J. Chem. Theory Comput.* **2010**, *359*–369. (b) Wang, B.; Truhlar, D. G. Geometry optimization using tuned and balanced redistributed charge schemes for combined quantum mechanical and molecular mechanical calculations. *Phys. Chem. Chem. Phys.* **2011**, *13* (22), 10556–10564. (c) Wang, B.; Truhlar, D. G. Tuned and balanced redistributed charge scheme for combined quantum mechanical and molecular mechanical (QM/MM) methods and fragment methods: Tuning based on the CMS charge model. *J. Chem. Theory Comput.* **2013**, *9*, 1036–1042.
- (10) Salomon-Ferrer, R.; Case, D. A.; Walker, R. C. An overview of the Amber biomolecular simulation package. *Wiley Interdiscip. Rev.: Comput. Mol. Sci.* **2013**, *3* (2), 198–210.
- (11) Brooks, B. R.; Brooks, C. L., III; Mackerell, A. D.; Nilsson, L.; Petrella, R. J.; Roux, B.; Won, Y.; Archontis, G.; Bartels, C.; Boresch, S.; Caflisch, A.; Caves, L.; Cui, Q.; Dinner, A. R.; Feig, M. CHARMM: The biomolecular simulation program. *J. Comput. Chem.* **2009**, *30*, 1545–1614.
- (12) Field, M. J. The pDynamo program for molecular simulations using hybrid quantum chemical and molecular mechanical potentials. *J. Chem. Theory Comput.* **2008**, *4* (7), 1151–1161.
- (13) Scott, W. R. P.; Hünenberger, P. H.; Tironi, I. G.; Mark, A. E.; Billeter, S. R.; Fennen, J.; Torda, A. E.; Huber, T.; Krüger, P.; van Gunsteren, W. F. The GROMOS biomolecular simulation program package. *J. Phys. Chem. A* **1999**, *103* (19), 3596–3607.
- (14) Amara, P.; Field, M. J. Evaluation of an ab initio quantum mechanical/molecular mechanical hybrid-potential link-atom method. *Theor. Chem. Acc.* **2003**, *109* (1), 43–52.
- (15) Frisch, M. J.; Trucks, G. W.; Schlegel, H. B.; Scuseria, G. E.; Robb, M. A.; Cheeseman, J. R.; Scalmani, G.; Barone, V.; Mennucci, B.; Petersson, G. A.; Nakatsuji, H.; Caricato, M.; Li, X.; Hratchian, H. P.; Izmaylov, A. F.; Bloino, J.; Zheng, G.; Sonnenberg, J. L.; Hada, M.; Ehara, M.; Toyota, K.; Fukuda, R.; Hasegawa, J.; Ishida, M.; Nakajima, T.; Honda, Y.; Kitao, O.; Nakai, H.; Vreven, T.; Montgomery, J. A., Jr.; Peralta, J. E.; Ogliaro, F.; Bearpark, M.; Heyd, J. J.; Brothers, E.; Kudin, K. N.; Staroverov, V. N.; Kobayashi, R.; Normand, J.; Ragahavachari, K.; Rendell, A.; Burant, J. C.; Iyengar, S. S.; Tomasi, J.; Cossi, M.; Rega, N.; Millam, J. M.; Klene, M.; Knox, J. E.; Cross, J. B.; Bakken, V.; Adamo, C.; Jaramillo, J.; Gomperts, R.; Stratmann, R. E.; Yazayev, O.; Austin, A. J.; Cammi, R.; Pomelli, C.; Ochterski, J. W.; Martin, R. L.; Morokuma, K.; Zakrzewski, V. G.; Voth, G. A.; Salvador, P.; Dannenberg, J. J.; Dapprich, S.; Daniels, A. D.; Farkas, Ö.; Foresman, J. B.; Ortiz, J. V.; Cioslowski, J.; Fox, D. J. *Gaussian 09, Revision D.01*; Gaussian Inc.: Wallingford, CT, 2009.
- (16) Lin, H.; Truhlar, D. G. Redistributed charge and dipole schemes for combined quantum mechanical and molecular mechanical calculations. *J. Phys. Chem. A* **2005**, *109* (17), 3991–4004.
- (17) MacKerell, A. D.; Bashford, D.; Bellott, M.; Dunbrack, R. L.; Evanseck, J. D.; Field, M. J.; Fischer, S.; Gao, J.; Guo, H.; Ha, S.; Joseph-McCarthy, D.; Kuchnir, L.; Kuczera, K.; Lau, F. T. K.; Mattos, C.; Michnick, S.; Ngo, T.; Nguyen, D. T.; Prodhom, B.; Reiher, W. E.; Roux, B.; Schlenkrich, M.; Smith, J. C.; Stote, R.; Straub, J.; Watanabe, M.; Wiorkiewicz-Kuczera, J.; Yin, D.; Karplus, M. All-atom empirical potential for molecular modeling and dynamics studies of proteins. *J. Phys. Chem. B* **1998**, *102* (18), 3586–3616.
- (18) Jorgensen, W. L.; Tirado-Rives, J. The OPLS [optimized potentials for liquid simulations] potential functions for proteins, energy minimizations for crystals of cyclic peptides and crambin. *J. Am. Chem. Soc.* **1988**, *110*, 1657–1666.
- (19) Cazet, A.; Julien, S.; Bobowski, M.; Burchell, J.; Delannoy, P. Tumour-associated carbohydrate antigens in breast cancer. *Breast Cancer Res.* **2010**, *12* (3), 204.
- (20) (a) Yang, Y.; Yu, H.; York, D.; Cui, Q.; Elstner, M. Extension of the self-consistent-charge density-functional tight-binding method: Third-order expansion of the density functional theory total energy and introduction of a modified effective Coulomb interaction. *J. Phys. Chem. A* **2007**, *111*, 10861–10873. (b) Gaus, M.; Cui, Q.; Elstner, M. DFTB3: Extension of the self-consistent-charge density-functional tight-binding method (SCC-DFTB). *J. Chem. Theory Comput.* **2011**, *7*, 931–948.
- (21) (a) Govender, K. K.; Gao, J.; Naidoo, K. J. Reoptimization of carbon parameters for AM1/d-PhoT to improve ring pucker of glucose. Unpublished. (b) Nam, K.; Cui, Q.; Gao, J.; York, D. M. Specific reaction parametrization of the AM1/d Hamiltonian for phosphoryl transfer reactions: H, O, and P atoms. *J. Chem. Theory Comput.* **2007**, *3*, 486–504.
- (22) Vanommeslaeghe, K.; Hatcher, E.; Acharya, C.; Kundu, S.; Zhong, S.; Shim, J.; Darian, E. CHARMM general force field: A force field for drug-like molecules compatible with the CHARMM all-atom additive biological force fields. *J. Comput. Chem.* **2009**, *31*, 671–690.
- (23) Kuttel, M.; Brady, J. W.; Naidoo, K. J. Carbohydrate solution simulations: producing a force field with experimentally consistent primary alcohol rotational frequencies and populations. *J. Comput. Chem.* **2002**, *23* (13), 1236–1243.
- (24) Thiel, W. MNDO97, version 5.0; University of Zurich: Zurich, Switzerland, 1998.
- (25) Jorgensen, W. L.; Chandrasekhar, J.; Madura, J. D.; Impey, R. W.; Klein, M. L. Comparison of simple potential functions for simulating liquid water. *J. Chem. Phys.* **1983**, *79* (2), 926–935.
- (26) van Gunsteren, W. F.; Berendsen, H. J. C. Algorithms for macromolecular dynamics and constraint dynamics. *Mol. Phys.* **1977**, *34*, 1311–1327.
- (27) Cui, Q.; Elstner, M.; Kaxiras, E.; Frauenheim, T.; Karplus, M. A QM/MM implementation of the self-consistent charge density functional tight binding (SCC-DFTB) method. *J. Phys. Chem. B* **2001**, *105*, 569–585.
- (28) Pu, J. Z.; Gao, J. L.; Truhlar, D. G. Combining self-consistent-charge density-functional tight-binding (SCC-DFTB) with molecular

mechanics by the generalized hybrid orbital (GHO) method. *J. Phys. Chem. A* **2004**, *108* (25), 5454–5463.

(29) Konig, P. H.; Hoffmann, M.; Frauenheim, T.; Cui, Q. A critical evaluation of different QM/MM frontier treatments with SCC-DFTB as the QM method. *J. Phys. Chem. B* **2005**, *109* (18), 9082–9095.

(30) Goldberg, D. *Genetic Algorithms in Search, Optimization and Machine Learning*; Addison-Wesley: Reading, MA, 1989.

(31) Reuter, N.; Dejaegere, A.; Maigret, B.; Karplus, M. Frontier bonds in QM/MM methods: A comparison of different approaches. *J. Phys. Chem. A* **2000**, *104*, 1720–1735.